

# In Situ Synthesis of Gold and Silver Nanoparticles by Using Redox-Active Amphiphiles and Their Phase Transfer to Organic Solvents

Satyabrata Si, Enakshi Dinda, and Tarun K. Mandal\*<sup>[a]</sup>

**Abstract:** An in situ reduction approach to synthesizing gold and silver nanoparticles by using a series of newly designed, redox-active amphiphiles at basic pH is described. These amphiphiles are the conjugates of a fatty acid (e.g., oleic acid, stearic acid, and lauric acid) and a redox-active amino acid (e.g., tryptophan or tyrosine). The amphiphile-coated nanoparticles are then efficiently transferred from water to different nonpolar organic media (such as benzene, toluene, xylene, cyclohex-

ane, and hexane) simply by acid treatment. The phase-transfer process was monitored by UV/visible spectroscopy and transmission electron microscopy, and the results showed that the average particle size and size distribution remain almost unchanged after transferring to the organic media. The an-

**Keywords:** amphiphiles • gold • nanoparticles • phase transfer • silver

choring of the amphiphile to the nanoparticle surface was confirmed by FTIR spectroscopy and thermogravimetric analysis. A mechanism is proposed to describe the stability of colloidal Au and Ag nanoparticles formed in situ and their phase transfer to organic solvents. The presence of the amphiphile increases the thermal stability of the colloidal gold nanoparticle conjugates in organic solvents.

## Introduction

The synthesis of noble metal nanoparticles (MNPs) has attracted the whole nano-community due to their intrinsic size- and shape-dependent optoelectronic properties. A variety of synthetic wet-chemical techniques have already been developed to prepare size- and shape-tunable MNPs, most of which are water-based methods.<sup>[1–5]</sup> However, the use of nonpolar organic media to synthesize noble MNPs has been

an important branch of nanoparticle (NP) research in recent years.<sup>[6]</sup> The importance of such MNPs is mainly due to their versatility in terms of their application as a catalyst for organic reactions in nonpolar media,<sup>[7,8]</sup> their solvent-dependent optical properties,<sup>[9,10]</sup> and also the binding ability of stabilizer molecules on to the surface of MNPs in contact with various environments.<sup>[11,12]</sup> Furthermore, MNPs in organic media are susceptible to spontaneous assembly into hexagonal-close-packed monolayers upon solvent evaporation, which eventually produces new structural materials.<sup>[13–15]</sup>

The methods for direct single-phase synthesis of MNPs in nonpolar organic media are limited because of the poor solubility of the corresponding metal-ion precursor. In particular, the synthesis of gold nanoparticles (GNPs) in nonpolar organic media (such as toluene, benzene, xylene, and cyclohexane) is very rare, maybe because of the commercial unavailability of soluble gold-ion precursors in these solvents. Among the few reports of organic-based MNP synthesis, most are generally based on the thermal treatment of a metal-ion precursor in the presence of a capping molecule in organic solvent.<sup>[16–20]</sup> These methods are restricted to only a few MNP syntheses, and thus a two-phase synthesis protocol is adopted for the organic-phase synthesis of MNPs. Brust et al. were the first to develop a two-step method for preparing MNPs in organic media, which involved the trans-

[a] Dr. S. Si, E. Dinda, Dr. T. K. Mandal  
Polymer Science Unit & Centre for Advanced Materials  
Indian Association for the Cultivation of Science  
Jadavpur, Kolkata 700 032 (India)  
Fax: (+91) 33-2473-2805  
E-mail: psutkm@mahendra.iacs.res.in



Supporting information for this article contains details of the synthesis and characterization of redox-active amphiphiles, a plot of surface tension against concentration of sodium salt for all the amphiphiles, UV/visible spectra of the Ole-Trp-GNPs conjugates with varying amounts of amphiphile, UV/visible spectra of the Ole-Tyr-GNPs conjugates in different organic solvents, UV/visible spectra of the Ole-Trp-GNPs conjugates in toluene after transfer by using different protonated acid, additional TEM images, histogram plot of the amphiphile-GNPs/SNPs conjugates in water and in toluene, DLS curves, FTIR spectra of Ole-Trp-GNPs conjugates, and the change of the SPR property of the amphiphile-GNPs/SNPs conjugates in toluene as function of temperature. This data is available on the WWW under <http://www.chemeurj.org/> or from the author.

fer of  $\text{HAuCl}_4$  from water to toluene by using a phase-transfer catalyst, tetraalkylammonium bromide, followed by reduction using sodium borohydride in the organic phase.<sup>[14]</sup> Consequently, the Brust protocol was rapidly followed by other researchers for preparing self-assembled monolayers (SAMs) of alkanethiol,<sup>[21,22]</sup> aromatic thiol,<sup>[23,24]</sup> alkyl amine,<sup>[15,25,26]</sup> dialkyl disulfide,<sup>[27]</sup> and thiolated cyclodextrin<sup>[28,29]</sup> molecules on GNP and silver nanoparticle (SNP) surfaces. However, the disadvantage of this method, as reported by Rao et al., is that the MNPs formed contain nitrogenous surface impurities due to the presence of phase-transfer reagent, which render it difficult to obtain good superstructures.<sup>[30]</sup> Sastry et al. have modified the two-step Brust protocol for the synthesis of organic-based MNPs to one step. In this method, the phase transfer of chloroaurate ions from water to chloroform, and their spontaneous reduction to yield stable GNPs of controllable size, was accomplished by a single molecule, such as hexadecylaniline.<sup>[31]</sup>

Another approach involves the direct transfer of preformed aqueous-based MNPs to the organic phase by using an appropriate chemical approach. This transfer process requires hydrophobization of the MNP surface.<sup>[6,26,32–36]</sup> Most of these techniques mainly differ due to the different nature of the capping molecule, which needs different chemistry to hydrophobize the surface of the NPs.<sup>[6]</sup> Underwood and Mulvaney were the first to transfer the preformed, citrate-capped GNPs from water to an organic solvent, such as butyl acetate.<sup>[37]</sup> A simple place-exchange method can also be used to transfer alkanethiol-capped GNPs to organic solvents.<sup>[38–40]</sup> Similarly, GNPs capped with alkyl amine can also be used to accomplish such phase transfer to organic media.<sup>[15,25,26,32,41,42]</sup> Rao and co-workers have demonstrated the HCl-assisted phase transfer of aqueous colloidal Au, Pt, and Ag NPs into organic solvents, such as toluene, by using alkanethiols.<sup>[30,43]</sup> Efrima et al. have reported the transfer of sodium oleate-capped SNPs from water to organic solvents by using a small amount of orthophosphoric/perchloric acid in the reaction medium, with a transfer efficiency of 50–70%.<sup>[11,12]</sup> However, other acids, such as  $\text{H}_2\text{SO}_4$ , HCl, formic acid, or anisic acid, did not induce such phase transfer. Sastry et al. have also reported the phase transfer of oleic acid-capped Ni/Ag core-shell NPs by using orthophosphoric/perchloric acid, but they were not successful with HCl/ $\text{H}_2\text{SO}_4$ .<sup>[44]</sup>

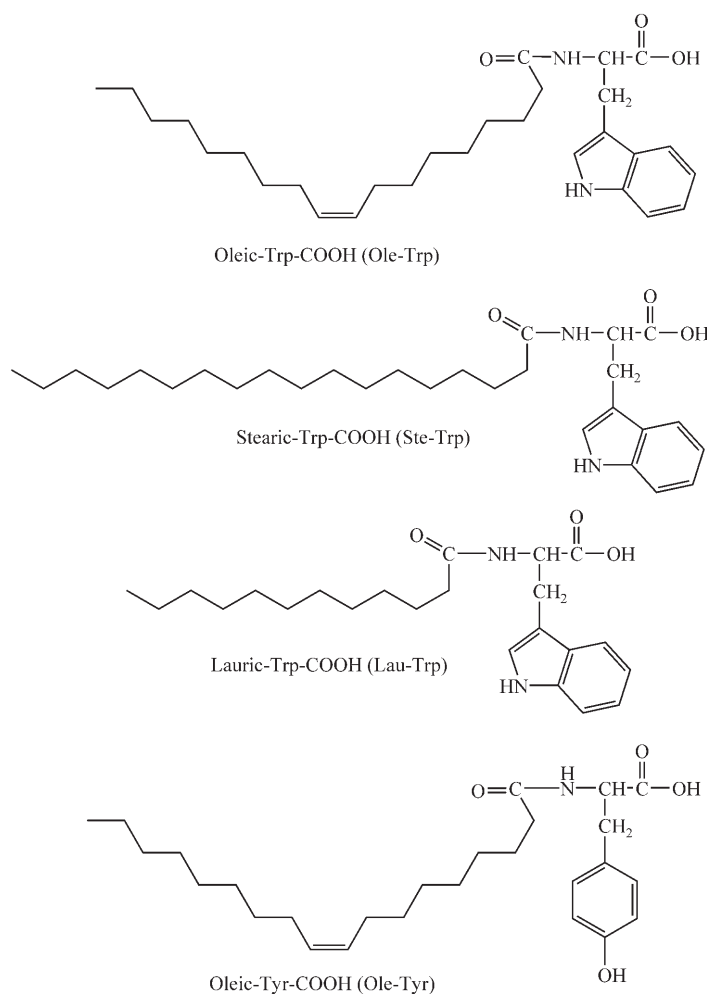
In situ synthetic methods for the generation of MNPs are gaining much interest, as they avoid the use of any external reducing agent or stabilizer.<sup>[45–48]</sup> Based on this technique, we have already reported the formation of gold and silver NPs by using the redox-active tyrosine/tryptophan-based peptides.<sup>[49–51]</sup> Sastry et al. have also reported the formation of GNPs by using alkylated tyrosine at the liquid/liquid and air/water interface.<sup>[52]</sup> To the best of our knowledge, except for this work, there are no reports on the in situ synthesis of gold and silver NPs in water by using redox-active amino acid based amphiphiles and their subsequent transfer to organic solvents.

Herein, we report the synthesis of colloidal gold and silver NPs by the in situ reduction technique at pH 11, by using a series of newly designed, redox-active amphiphiles as the reductant/stabilizer. These amphiphiles are the conjugate of a fatty acid (e.g., oleic acid, stearic acid, or lauric acid) and a redox-active amino acid (e.g., tryptophan or tyrosine). The MNPs formed are then efficiently transferred to different nonpolar organic solvents simply by acid treatment.

## Results and Discussion

### Redox-active amphiphile synthesis and characterization:

Redox-active amino acid based amphiphiles were synthesized by conventional solution-phase coupling of the respective amino acid and fatty acid by using a racemization-free fragmentation/condensation strategy, and the corresponding sodium salt was obtained by titration of the respective amphiphile with sodium hydroxide in ethanol according to the literature report.<sup>[53]</sup> Scheme 1 depicts the chemical structures of all the above-mentioned amphiphiles. Details of the syn-



Scheme 1.

thesis procedure and their characterization are provided in the Supporting Information. The amphiphiles exist as aggregated micellar structures in the aqueous alkaline phase, and micelle formation can be well understood from the surface tension data. The value of the critical micelle concentration (CMC) was determined from the slope of the surface tension versus concentration curve, and was found to be  $\approx 0.14$  mM for the sodium salt of the amphiphile Ole-Trp (see Figure S1 in the Supporting Information). Similarly, the CMCs of the sodium salt of amphiphiles Ste-Trp, Lau-Trp, and Ole-Tyr were calculated to be  $\approx 0.034$ ,  $\approx 0.163$ , and  $\approx 0.029$  mM, respectively.

**Synthesis of amphiphile–GNP and amphiphile–SNP conjugates:** In aqueous alkaline solution, the hydrophilic end of the amphiphile contains a carboxylate group along with an adjacent tryptophan or tyrosine moiety, whereas the hydrophobic part contains the long alkyl chain. Typically, an aqueous solution of  $\text{HAuCl}_4$  (0.5 mL, 10 mM) was added dropwise to the alkaline solution of each amphiphile (1 mL, 40 mM) separately at  $\text{pH} \approx 11$ . The UV/visible spectrum of this as-prepared Ole-Trp-gold nanoparticles (Ole-Trp–GNPs) conjugate in water exhibits a sharp surface plasmon resonance (SPR) band at 528 nm (Figure 1a). The UV/visible spectra of Ole-Trp–GNPs prepared with various amounts (1.0, 0.75, 0.5, 0.25 mL; 40 mM) of the amphiphile Ole-Trp and with a fixed amount (0.5 mL, 10 mM) of  $\text{Au}^{3+}$  is provided in Figure S2 of the Supporting Information. The optical results show that an increase in the amount of amphiphile only increases the intensity of the SPR band at 528 nm corresponding to the formed GNPs, indicating the formation of only spherical GNPs. Thus, all other reactions

were carried out with 1 mL of amphiphile (40 mM) and 0.5 mL of  $\text{Au}^{3+}$  ion (10 mM) as they yielded a higher number of GNPs. In all cases, we observed a color change from yellow to ruby red, indicating the formation of colloidal GNPs by oxidation of the tryptophan residue of the amphiphiles through electron transfer from the tryptophan moiety to the  $\text{Au}^{3+}$  ion, as reported in our earlier work.<sup>[49]</sup> The GNPs formed are stabilized by anchoring of the indole part of the tryptophan moiety of the amphiphiles. The details of the formation and stabilization mechanism of the nanoconjugates will be discussed later in this section. In the case of SNPs, the in situ reduction of  $\text{AgNO}_3$  by the tryptophan moiety of the amphiphile results in a color change from colorless to yellow, indicating the formation of colloidal amphiphile–SNPs conjugates that were similarly transferred to various organic solvents.

**Phase transfer:** The appearance of a single, sharp SPR band at 528 nm (Figure 1a) indicates the presence of well-dispersed GNPs of sizes below 20 nm.<sup>[54]</sup> After HCl treatment, the Ole-Trp–GNPs conjugate is completely transferred to toluene after stirring for just 1 min, and the corresponding absorption spectrum shows a sharp SPR band at 528 nm with much-enhanced intensity (Figure 1b). The UV/visible spectrum of the remaining aqueous phase shows no trace of any SPR signal of GNPs, indicating the complete transfer of the Ole-Trp–GNPs conjugate to the toluene phase (Figure 1c). This finding can be confirmed by the pictures of the Ole-Trp–GNPs conjugate in both aqueous and organic phases (see inset of Figure 1), which clearly shows that the color of the organic phase changes to ruby red while at the same time the aqueous phase becomes colorless. These results also reveal that there is no change in the position of the SPR band after the transfer of the Ole-Trp–GNPs conjugate to the organic phase. The enhancement in the intensity of the SPR band in toluene may be due to the change of polarity of the surrounding solvent of the GNPs as a result of the transfer from water to toluene.

Also, the Ole-Trp–GNPs conjugate is effectively transferred to other organic solvents, such as benzene, xylene, cyclohexane, and hexane, in a similar fashion and the UV/visible spectra are shown in Figure 2. In all cases, the spectra show that the SPR band of the GNPs remains at the same position at 528 nm before and after the transfer. The insets of Figure 2 display pictures of the colloidal Ole-Trp–GNPs conjugate in these solvents, showing the same color as observed in the case of the nanoconjugate in toluene.

To study the effect of alkyl chain length and the olefinic double bond on the preparation of GNPs and their transfer to organic media, we prepared GNPs by using two different amphiphiles (Ste-Trp and Lau-Trp; Scheme 1) following similar experimental conditions as those used for Ole-Trp, in which the oleyl chain of Ole-Trp is replaced by stearyl and lauryl chains, respectively. Both the experiments resulted in the formation of stable suspensions of GNPs in water, which were completely transferred to toluene upon acidification with HCl after just 1 min. Figure 3 shows the UV/visible

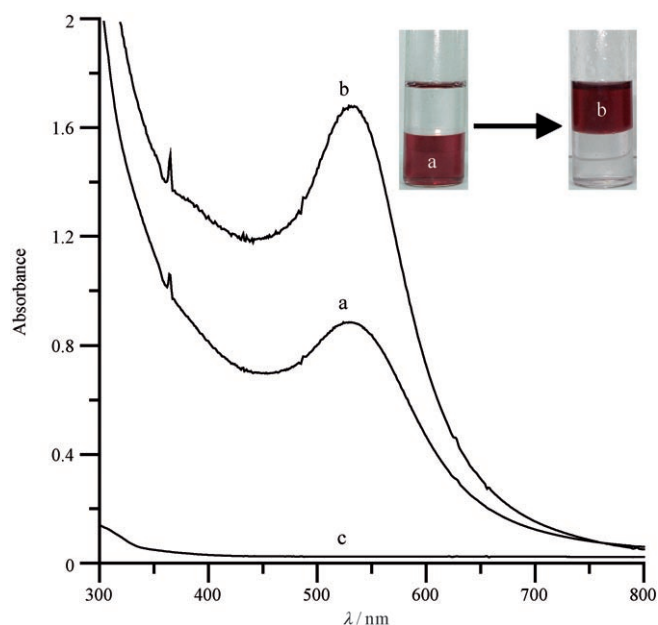


Figure 1. UV/visible absorption spectra of Ole-Trp–GNPs conjugate: a) as-prepared in water, b) after transferring to toluene, and c) the remaining aqueous layer after the transfer. Inset: pictures of the colloidal Ole-Trp–GNPs conjugate in two different phases.

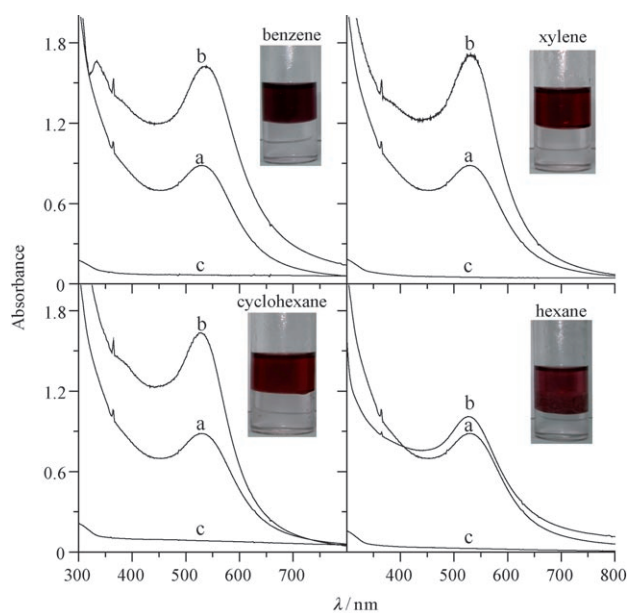


Figure 2. UV/visible absorption spectra of Ole-Trp-GNPs conjugate: a) as-prepared in water, b) after transferring to the respective organic solvents, and c) the remaining aqueous layer after the transfer. Insets: pictures of the colloidal Ole-Trp-GNPs conjugate in the respective organic solvents.

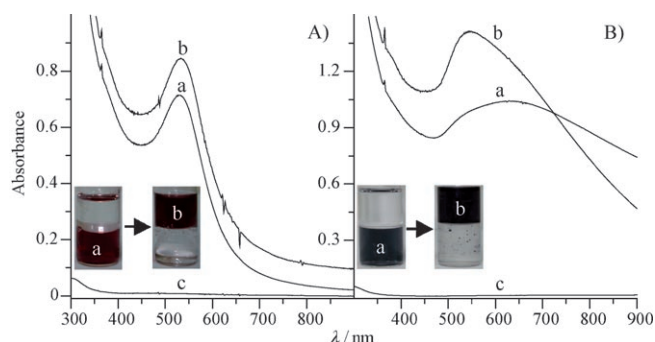


Figure 3. UV/visible absorption spectra of A) Lau-Trp-GNPs conjugate and B) Ste-Trp-GNPs conjugate: a) as-prepared in water, b) after transferring to toluene, and c) the remaining aqueous layer after the transfer. Insets: pictures of the colloidal GNP conjugates in two different media.

spectra of the Ste-Trp-GNPs and Lau-Trp-GNPs conjugates in water and after transferring them to toluene. These results indicate that the SPR band position of the Lau-Trp-GNPs conjugate in water and in toluene remains the same (528 nm) as that of the Ole-Trp-GNPs conjugate (compare Figures 1 and 3A). However, the as-prepared Ste-Trp-GNPs conjugate in water exhibits a broad SPR band centered at 629 nm (Figure 3Ba). The appearance of such a broad SPR band may be due to the formation of irregular-shaped particles of wide distribution or of aggregated GNPs, which will be confirmed by transmission electron microscopy (TEM) analysis later in this section. The Ste-Trp-GNPs suspension on shaking with toluene at pH 2–3 results in complete transfer to toluene with the SPR band centered at 545 nm (Figure 3Bb). The actual reason for this blue shift from 629 to

545 nm is not clear, but may be due to the better dispersibility of the Ste-Trp-GNPs conjugate in toluene compared to that in water. Because of the broad SPR band, we observe a blue suspension that changes to violet on transferring from the aqueous to the toluene phase.

Earlier, we reported the synthesis of gold and silver NPs by using tyrosine-containing peptides through electron transfer from the tyrosine residue to the metal ion.<sup>[50,51]</sup> This study further prompted us to design redox-active amphiphiles containing a tyrosine residue for GNP formation. Thus, the amphiphile oleic-Tyr-COOH (Ole-Tyr; Scheme 1) was utilized for preparing GNPs by using similar reaction conditions as those for the tryptophan-containing amphiphile-based synthesis. The UV/visible spectrum of the as-prepared Ole-Tyr-GNPs conjugate in water shows a SPR band at 521 nm (Figure 4a). The Ole-Tyr-GNPs conjugate

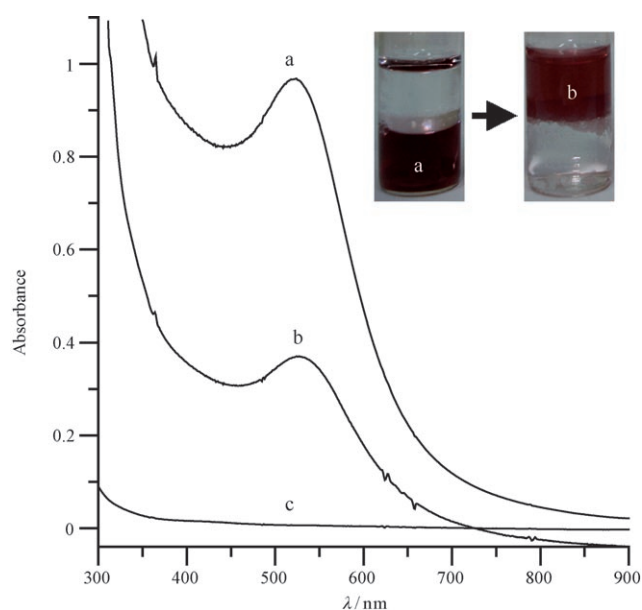


Figure 4. UV/visible absorption spectra of the Ole-Tyr-GNPs conjugate: a) as-prepared in water, b) after transferring to toluene, and c) the remaining aqueous layer after the transfer. Inset: pictures of the colloidal GNP conjugate in two different media.

was then treated with HCl in the presence of different non-polar organic solvents under vigorous magnetic stirring. The UV/visible spectrum shows no change in the SPR band position of the Ole-Tyr-GNPs conjugate after transferring to toluene (compare Figures 4a and 4b), but a decrease in intensity of the SPR band is observed, which may be due to the poor solubility of the base amphiphile, Ole-Tyr, in toluene. The Ole-Tyr is partially soluble in benzene, toluene, and xylene, whereas it is insoluble in cyclohexane and hexane. The Ole-Tyr-GNPs conjugate was thus partially transferred to benzene, toluene, and xylene, but not to cyclohexane or hexane. The UV/visible spectra of the Ole-Tyr-GNPs conjugate in different organic solvents show the presence of a SPR band of GNPs at 521 nm after transferring to benzene and xylene, but no such band is observed in



cyclohexane and hexane (see Figure S3 in the Supporting Information). Thus, the presence of a tyrosine-based amphiphile also enables transfer of GNPs to nonpolar organic solvents because of the anchoring of the tyrosine OH group of the Ole-Trp to the GNP surface, as reported earlier.<sup>[50]</sup>

To study the versatility of this method, SNPs were also prepared by the reduction of  $\text{AgNO}_3$  by using the amphiphile Ole-Trp under similar reaction conditions. The aqueous suspension of Ole-Trp-SNPs conjugates was then allowed to transfer to toluene by treatment with HCl. Figure 5 shows the UV/visible spectra of the Ole-Trp-SNPs conjugate in water and toluene. These optical results indicate the complete transfer of SNPs to the toluene layer, but the SPR band position was slightly red-shifted from 417 to 421 nm (compare Figures 5a and 5b) upon transferring from water to toluene. The inset of Figure 5 displays pictures of colloidal Ole-Trp-SNPs in water and in toluene, showing complete transfer of SNPs. We have also successfully transferred the Ole-Trp-SNPs conjugates into other organic solvents, such as benzene, xylene, hexane, and cyclohexane.

Our method of phase transfer is not restricted to any particular acid treatment, and other protonated acids, such as  $\text{H}_2\text{SO}_4$ ,  $\text{HCOOH}$ , and  $\text{H}_3\text{PO}_4$ , are also capable of effectively transferring the amphiphile-MNPs conjugates to various nonpolar organic solvents. This is clearly evident from the appearance of a sharp SPR band in the UV/visible spectra of the Ole-Trp-GNPs conjugate in toluene by using different protonated acids (see Figure S4 in the Supporting Information). As we are able to transfer these amphiphile-GNPs/SNPs by using any protonated acid, this method is superior to other similar methods<sup>[11–13,44]</sup> and can be applied to the transfer of a wide range of noble MNPs.

Figure 6A shows a TEM image of the as-prepared Ole-Trp-GNPs conjugate in water, indicating well-dispersed spherical NPs; the average size was calculated to be  $7.4 \pm 1.3$  nm, taking at least 100 particles into consideration. The TEM picture of this conjugate in toluene also shows spherical particles of average size  $7.5 \pm 1.3$  nm (Figure 6B). Figures 6C and 6D show a histogram analysis of the particle size distribution of the corresponding Ole-Trp-GNPs conjugates in

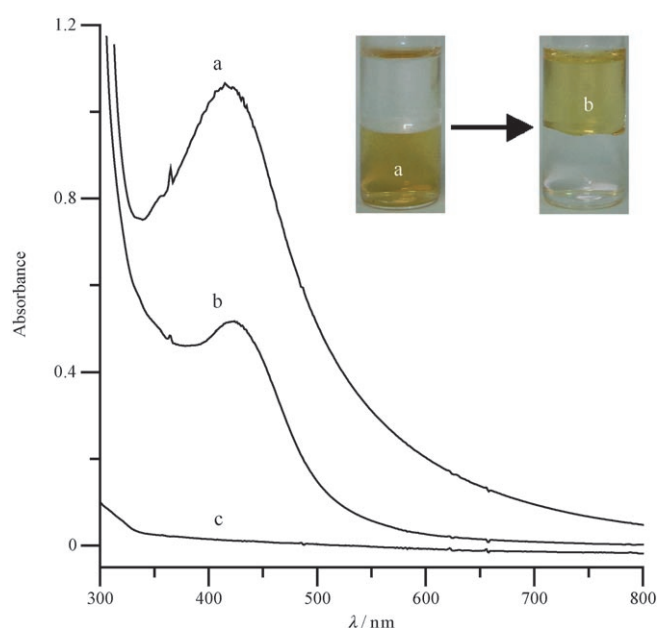


Figure 5. UV/visible absorption spectra of the Ole-Trp-SNPs conjugate: a) as-prepared in water, b) after transferring to toluene, and c) the remaining aqueous layer after the transfer. Inset: pictures of the colloidal SNP conjugate in water and in toluene.

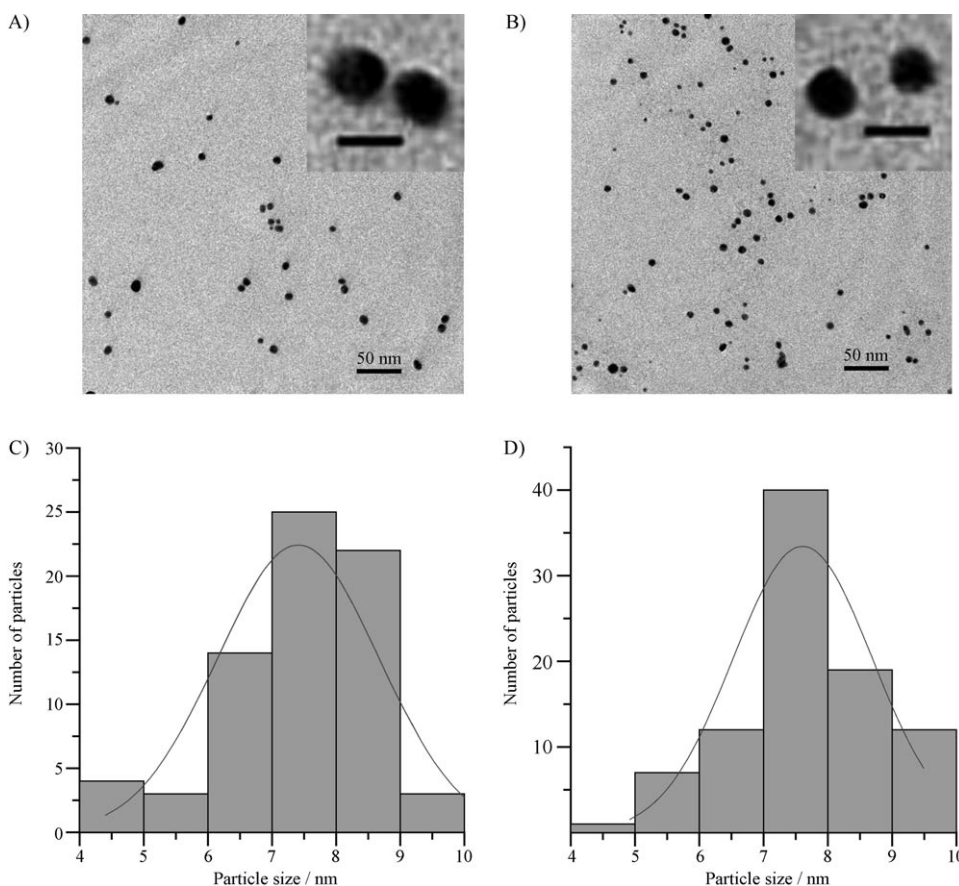


Figure 6. TEM images of the Ole-Trp-GNPs conjugate: A) as-prepared in water and B) after transferring to toluene. Insets: enlarged views of the corresponding images; scale bars: 10 nm. Histograms of particle size distribution analyzed from the corresponding TEM images of the conjugate: C) as-prepared in water and D) after transferring to toluene.

aqueous and toluene phases, respectively. These results indicate that the particle size and the size distribution remain almost unaltered on transfer from water to toluene. Thus, we can conclude that the transfer process brings no change in the GNPs' morphology and size distribution.

Figure 7 shows the corresponding TEM images of the Ste-Trp-GNPs, Lau-Trp-GNPs, Ole-Tyr-GNPs, and Ole-Trp-SNPs conjugates in water and in toluene. From the TEM pictures, it is evident that the Ste-Trp-GNPs conjugate has no definite shape, whereas the morphologies of Lau-Trp-

GNPs, Ole-Tyr-GNPs, and Ole-Trp-SNPs conjugates are all spherical in nature in the aqueous phase. The formation of such irregular-shaped Ste-Trp-capped GNPs might result in the appearance of a broad SPR band as mentioned above (see Figure 3B). The blue shift of this band after transferring to the toluene phase might be due to the better dispersibility of the GNPs in toluene compared to that in the aqueous phase, as evident from Figures 7A and 7B. After transferring the respective particles to toluene, the average size and size distribution remain almost the same. The details of particle sizes of the NPs prepared with all four amphiphiles in both media are summarized in Table 1. Additional TEM images

Table 1. Particle size analysis of GNPs/SNPs determined from the respective TEM images.

GNPs/SNPs	Particle size in water [nm]	Particle size in toluene [nm]
Ole-Trp-GNPs	$7.4 \pm 1.3$	$7.5 \pm 1.3$
Ste-Trp-GNPs	—[a]	—[a]
Lau-Trp-GNPs	$6.8 \pm 0.6$	$6.8 \pm 0.5$
Ole-Tyr-GNPs	$6.7 \pm 1.3$	$7.0 \pm 1.2$
Ole-Trp-SNPs	$17.2 \pm 3.5$	$17.1 \pm 3.7$

[a] Unable to determine the size because of irregular-shaped particles.

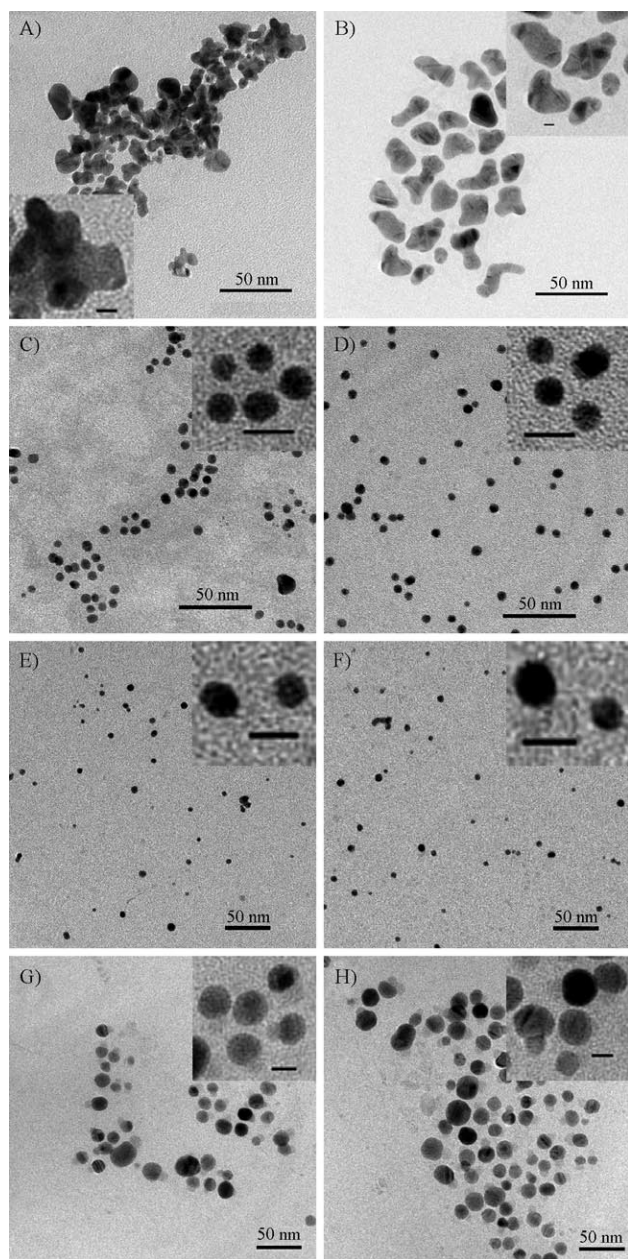


Figure 7. TEM images of A) Ste-Trp-GNPs conjugate in water, B) Ste-Trp-GNPs conjugate in toluene, C) Lau-Trp-GNPs conjugate in water, D) Lau-Trp-GNPs conjugate in toluene, E) Ole-Tyr-GNPs conjugate in water, F) Ole-Tyr-GNPs conjugate in toluene, G) Ole-Trp-SNPs conjugate in water, and H) Ole-Trp-SNPs conjugate in toluene. Insets: enlarged views of the corresponding TEM images; scale bars: 10 nm.

and the corresponding histogram analysis are provided in the Supporting Information (see Figures S5 and S6). As the shape of the Ste-Trp-GNPs conjugate is irregular in nature, we are unable to determine the exact size or the histogram. These results again indicate that the transfer of the GNPs/SNPs from the aqueous to the organic phase brings no change in the particle morphology and its distribution. However, from the particle size data reported in Table 1, we can summarize that as the alkyl chain length of the amphiphile decreases, the size of the GNPs formed decreases. Also, upon comparing the standard deviation values, one can conclude that the GNPs' size distribution tends more towards monodispersity.

To provide further support to the TEM analysis data, a dynamic light scattering (DLS) experiment was carried out to measure the particle size of a representative sample, Ole-Trp-GNPs conjugate, in water and in toluene. In the aqueous phase, the diameter of the Ole-Trp-GNPs conjugate was around 10.1 nm (see Figure S7 in the Supporting Information), which is very close to the value obtained from TEM measurements ( $7.4 \pm 1.3$  nm). Besides the peak for this particle size, another peak was also observed at 91.3 nm in the DLS curve. However, the TEM result shows no sign of any such large particle size throughout the grid. This may be due to the formation of a large cluster of individual GNPs in the aqueous phase or the micelle of the amphiphile, Ole-Trp, which may be destroyed during the drying of the sample on the TEM grid. The DLS study of GNPs in toluene indicates only one peak corresponding to a diameter of 7.5 nm, which also agrees well with the TEM result (see Table 1). The diameter of Ole-Trp-GNPs in water, as measured by DLS, is a little bigger compared to that of the TEM results, which may be due to the surrounding water

molecules associated with these NPs in the aqueous phase.<sup>[55]</sup>

**Evidence of amphiphile adsorption:** FTIR spectra of the neat Ole-Trp, neat sodium salt of Ole-Trp, and the centrifuged Ole-Trp–GNPs conjugate isolated from the aqueous and toluene phases are provided in the Supporting Information (see Figure S8) and the details of the peak assignment are summarized in Table 2. For both Ole-Trp and the sodium salt of Ole-Trp, bands at 2926 and 2854 cm<sup>-1</sup> were observed as a result of the asymmetric and symmetric stretching of the CH<sub>2</sub> groups. A band due to the stretching mode of the olefinic =C–H bond was also observed at 3007 cm<sup>-1</sup>. In addition, the Ole-Trp shows a band at 1728 cm<sup>-1</sup> due to the C=O stretching vibration, whereas the sodium salt of Ole-Trp shows bands at 1589 and 1406 cm<sup>-1</sup> due to asymmetric and symmetric COO<sup>-</sup> stretching frequencies, respectively. Both the above amphiphiles also show the amide I and II bands which appear in the regions 1650–1630 and 1530–1515 cm<sup>-1</sup>. The Ole-Trp–GNPs conjugate in both media shows the presence of the CH<sub>2</sub> vibration mode (2926 and 2854 cm<sup>-1</sup>), indicating the presence of the amphiphile on the GNP surface. The position of the olefinic =C–H bond vibration remains unchanged even after adsorption of the amphiphile to the surface of the GNPs, which indicates that the olefinic bond has no role in stabilizing the GNPs.

Earlier, it was reported that the stabilization of SNPs is achieved by the anchoring of oleic acid onto the surface through the interaction of its olefinic bond, and hence a shift in the olefinic vibration mode was observed.<sup>[12]</sup> The amphiphile Ole-Trp attached to the GNPs, isolated from aqueous phase, shows bands at 1589 and 1402 cm<sup>-1</sup>, indicating the presence of a carboxylate ion and not the carboxylic acid form. The amphiphile Ole-Trp attached to the GNPs shows bands at 1589 and 1402 cm<sup>-1</sup> in the aqueous phase, indicating the presence of a carboxylate ion and not the carboxylic acid form. A band appears at 1728 cm<sup>-1</sup> when it is transferred to the organic phase by acid treatment, indicating complete protonation of the carboxylate group present in the aqueous phase. Also, the Ole-Trp–GNPs conjugate in both the aqueous and organic phases shows the presence of amide I and II bands (1650–1630 and 1530–1515 cm<sup>-1</sup>). FTIR spectra of Ole-Trp–SNPs and the GNP conjugates prepared with the other amphiphiles also show a similar

type of band, as discussed above, and hence no data are provided for the sake of brevity. This result proves that the amphiphile molecules are really attached to the surface of the NPs.

The anchoring of the amphiphile on the surface of the NPs was further confirmed by the thermogravimetric analysis (TGA) of a representative sample, Ole-Trp–GNPs conjugate, isolated from two different media. Thermograms of the centrifuged/washed Ole-Trp–GNPs conjugates isolated

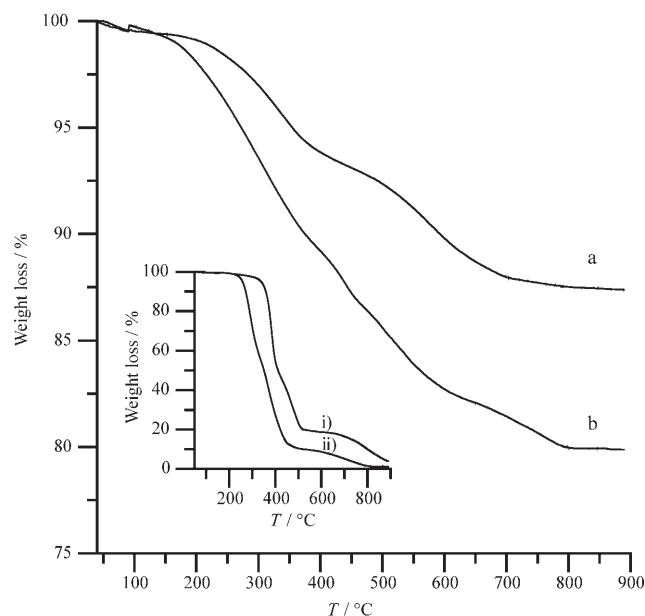


Figure 8. TGA thermogram of isolated Ole-Trp–GNPs conjugates from: a) water and b) toluene. Inset: TGA thermogram of neat i) sodium salt of Ole-Trp and ii) Ole-Trp.

from both water and toluene (Figure 8) were compared with those of the neat Ole-Trp and neat sodium salt of Ole-Trp (see inset of Figure 8). According to the thermograms, the onset of decomposition of the neat sodium salt of Ole-Trp and neat Ole-Trp is ≈350 [(i), inset of Figure 8] and ≈250°C [(ii), inset of Figure 8], respectively. However, the Ole-Trp–GNPs conjugate isolated from water starts decomposing at ≈240°C and the same nanoconjugate isolated from toluene starts decomposing at ≈190°C, which indicates

that GNPs promote decomposition of the amphiphile. The fact is that the amphiphile present in the as-prepared nanoconjugate isolated from water exists in the form of the sodium salt, whereas the amphiphile present in the same nanoconjugate after transferring to toluene exists in the acid form. As mentioned above, the decomposition temperature of the two forms of

Table 2. FTIR peak assignment of the amphiphile (Ole-Trp) and Ole-Trp–GNPs conjugate under different conditions.

Ole-Trp [cm <sup>-1</sup> ]	Sodium salt of Ole-Trp [cm <sup>-1</sup> ]	Ole-Trp–GNPs isolated from water [cm <sup>-1</sup> ]	Ole-Trp–GNPs isolated from toluene [cm <sup>-1</sup> ]	Peak assignment
3415	3412	3412	3405	indole NH
3007	3007	3007	3007	=C–H
2926, 2854	2926, 2854	2924, 2854	2924, 2852	CH <sub>2</sub>
1728	–	–	1728	C=O
–	1589, 1406	1589, 1402	–	COO <sup>-</sup>
1651, 1519	1630, 1527	1626, 1529	1651, 1521	amide I+II



the amphiphile are different; thus, this is the reason for the difference in the decomposition temperature of the adsorbed amphiphile on the surface of the GNPs isolated from water and toluene. Furthermore, the weight loss of the nanoconjugate isolated from water was calculated to be  $\approx 11\%$  between  $\approx 240$  and  $800^\circ\text{C}$  (Figure 8b), which is solely due to the decomposition of adsorbed amphiphile on the GNPs' surface. However, such a weight loss is  $\approx 19\%$  for the same nanoconjugate isolated from the toluene phase in the temperature range of 190 to  $800^\circ\text{C}$  (Figure 8b). These results confirm that the nature and the amount of amphiphile adsorbed on the surface of the GNPs are different, which leads to different modes of stabilization of GNPs by amphiphiles in the aqueous and toluene phases.

**Control experiments:** A control experiment was performed to explain the role of the tryptophan/tyrosine residue in the transfer of gold and silver NPs to the organic phase. GNPs were first prepared by the reduction of  $\text{HAuCl}_4$  with  $\text{NaBH}_4$  in the presence of neat oleic acid at pH 11. The UV/visible absorption spectrum shows the appearance of a sharp SPR band at 520 nm (Figure 9a), indicating well-dispersed GNPs that are stabilized within the oleic acid micelle. However, we were not able to transfer the GNPs to any nonpolar organic solvent, although we carried out the transfer process in a similar fashion to that discussed earlier. In this case, the toluene layer did not show any SPR band corresponding to GNPs (Figure 9b). Rather, the GNPs came out from the aqueous phase and stuck to the surface of the glass container at the interface of the two immiscible liquids. As a result, we did not observe any SPR signal in the remaining aqueous phase. A possible reason is that the GNPs formed are stabi-

lized within the micelle of oleic acid in the aqueous alkaline phase, as the oleic acid has no specific anchoring site for the GNPs' surface. When these oleate ion-capped GNPs are treated with an acid to transfer them to toluene, the micellar structure is disturbed because of the protonation of the carboxylate group of the oleate ion, and the GNPs are not able to stay in suspension. This results in aggregation of the GNPs and the aggregated particles separate out from toluene and stick to the surface of the glass container, as no specific anchoring group for the GNPs is present in the oleic acid molecule. From these results, we can conclude that the presence of a tryptophan/tyrosine residue in the amphiphile of oleic acid imparts extra stability to the formed colloidal GNPs and SNPs that can facilitate the easy transfer of these NPs from the aqueous to nonaqueous phase.

The control experiment also shows that the oleic acid capped SNPs cannot be transferred to the organic phase by using HCl. Similar observations have also been noticed by earlier researchers regarding the transfer of oleic acid capped SNPs.<sup>[12]</sup>

**Proposed mechanism:** On the basis of the above results, we propose the following mechanism for the formation, stabilization, and transfer of GNPs/SNPs to the organic phase. As a representative case, we have chosen the  $\text{HAuCl}_4$ /Ole-Trp system to explain the whole mechanism. In the aqueous phase, the tryptophan moiety of the amphiphile (Ole-Trp) reduces  $\text{Au}^{\text{III}}$  to metallic Au, which eventually makes clusters to form the GNPs and is stabilized by the micelle of Ole-Trp, as shown in Scheme 2. The NH group of the indole moiety of the tryptophan residue remains anchored to the GNP surface due to its reasonable binding efficiency, as reported in our earlier work.<sup>[49]</sup> The carboxylate group of the adsorbed amphiphile is protonated upon acidification with dilute HCl and becomes insoluble in the aqueous phase but soluble in the organic phase, and thus the protonated amphiphiles are readily transferred to the organic phase along with the anchored GNPs (Scheme 2). In a nonpolar organic phase the micelle structure is disturbed, but the amphiphile is still anchored to the surface of the GNPs through the tryptophan moiety and gives rise to stable dispersions of GNPs. The anchoring of the acid form of the amphiphile was evident from FTIR (Table 2) and TGA data (Figure 8). During acidification, intermolecular hydrogen bonding cannot be ruled out, which may result in self-assembly of amphiphile–GNPs conjugates, as reported in earlier research.<sup>[56]</sup> However, our TEM result did not show any such kind of assembly. We reasoned that the presence of long hydrophobic alkyl chains on the surface hinders the formation of self-assembled Ole-Trp–GNPs through hydrogen-bonding interactions. To prove this, the as-prepared Ole-Trp–GNPs conjugate was acidified with dilute HCl solution in the absence of toluene, which resulted in bulk precipitation due to insolubility of the amphiphile in water. On making the medium alkaline, the Ole-Trp–GNPs conjugate again formed a stable dispersion without any change in SPR band position. A similar type of mechanism is also valid for the

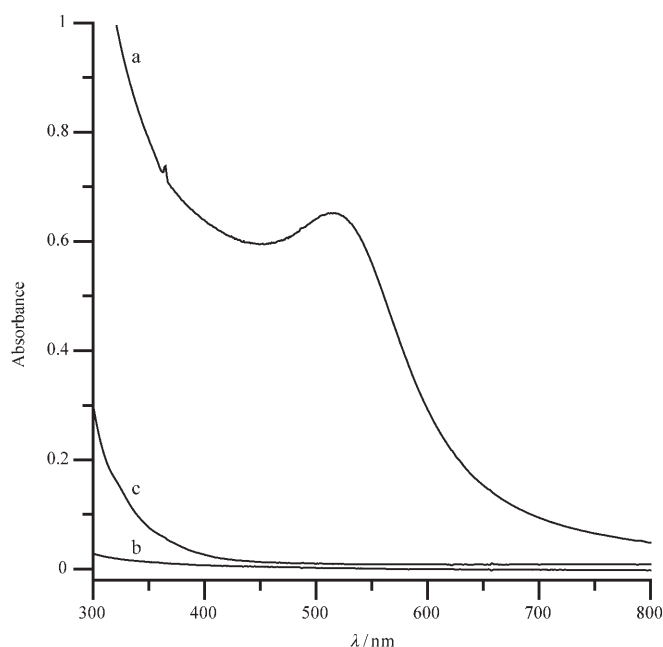
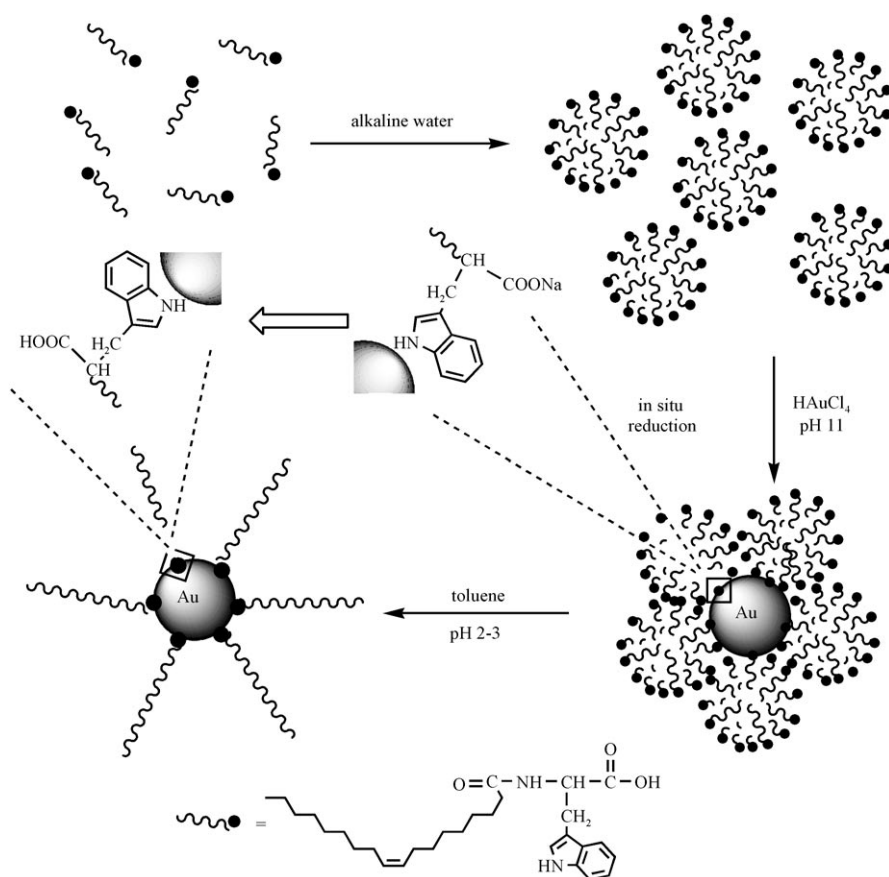


Figure 9. UV/visible absorption spectra of oleic acid capped GNPs: a) as-prepared in water, b) after transferring to toluene, and c) the remaining aqueous layer after the transfer.





Scheme 2.

remaining amphiphile-capped GNPs as well as amphiphile-capped SNPs.

**Reversibility study:** We also tried the switching of amphiphile-coated GNPs and SNPs between aqueous and organic phases repeatedly by changing the pH. The transfer occurs with 100% efficiency in the first cycle, that is, from aqueous to organic phase, whereas no transfer occurs in the second cycle, that is, from organic to aqueous phase. To resolve this issue in more detail, we tried the experiment with the neat amphiphile molecules (no GNPs or SNPs). The transfer occurred from the aqueous to the organic phase but not the reverse, as monitored by the UV/visible spectra of the tryptophan-containing amphiphile. This is probably due to the fact that in the aqueous phase the amphiphiles remain in the form of micelles, in which the hydrophobic chain is inside the core and the hydrophilic part is exposed to water. In this micellar solution, the GNPs or SNPs formed are stabilized through the anchoring of the tryptophan group adjacent to the carboxylate group (hydrophilic part) of the amphiphile (see Scheme 2). Thus, the carboxylate groups are exposed and can be readily protonated by acid treatment, which eventually promotes GNPs or SNPs to transfer to the organic phase. However, in the organic phase the hydrophilic carboxylic acid group of the amphiphile is at the core (nearer to the surface of the GNPs or SNPs) and is surrounded by a

layer of long hydrophobic alkyl chains, which prevents the aqueous alkali from entering the core. Thus, the attached carboxylic groups are not deprotonated by treatment with aqueous alkali, and the transfer of GNPs or SNPs to the aqueous phase is not possible.

**Thermal stability:** To study the effect of temperature on the stability of the colloidal amphiphile-GNPs in two different phases, we recorded the UV/visible spectra of the Ole-Trp-GNPs conjugate at varying temperatures and times before and after the transfer process. The SPR band of the Ole-Trp-GNPs conjugate in water is unchanged up to 80°C and remains stable for more than 2 h at that temperature (Figure 10A). After transferring to toluene, the intensity of the SPR band decreases slightly on increasing the temperature to 80°C and reverses back on cooling, which may be attributed to the change in refractive

index of toluene with temperature. Again, the Ole-Trp-GNPs conjugate was kept in toluene at 80°C in a thermostatic temperature bath and the SPR band was recorded at various time intervals. The spectra demonstrate that the Ole-Trp-GNPs conjugate is stable for more than 2 h at that temperature (Figure 10B). The SPR band of GNPs remains unaltered even if the heating (at 80°C) is prolonged for more than 12 h (Figure 10B). This result indicates that the colloidal Ole-Trp-GNPs conjugate is thermally (80°C) stable for more than 12 h in toluene, unlike the alkyl thiol-capped MNPs, which undergo irreversible change just above 60°C.<sup>[57,58]</sup> The higher thermal stability of the amphiphile-GNPs conjugates allows one to effectively use these GNPs for the fabrication of various optoelectronic devices. The other amphiphile-GNPs/SNPs suspensions are also stable against temperature and the details are provided in the Supporting Information (see Figure S9).

## Conclusion

A series of newly designed amphiphiles, with either a redox-active tryptophan or tyrosine moiety at one terminus, was successfully used for the preparation of gold and silver NPs by the in situ reduction technique at basic pH. An efficient method was developed for complete transfer of gold and

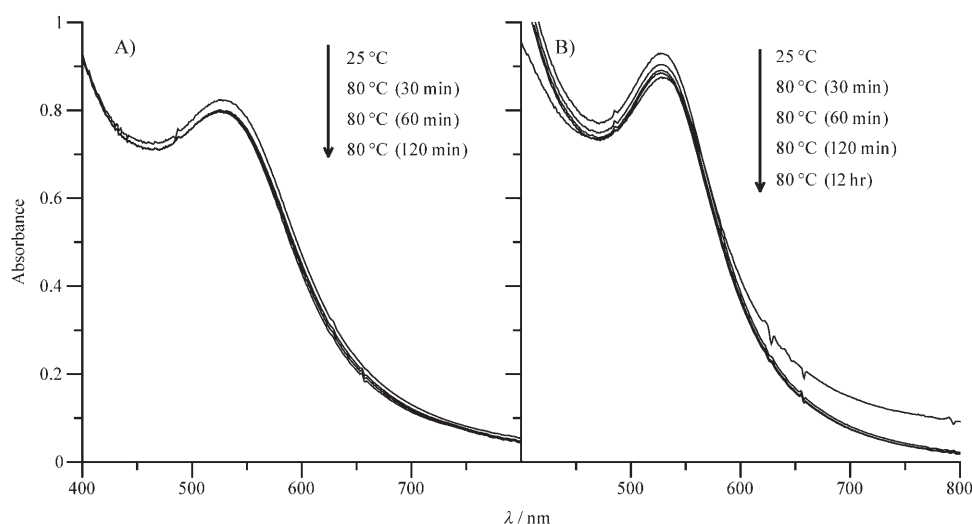


Figure 10. UV/visible absorption spectra of the Ole-Trp-GNPs conjugate as a function of temperature in A) water and B) toluene.

silver NPs to various nonpolar organic solvents without causing any particle aggregation, simply by changing the pH of the medium from alkaline to acidic. The UV/visible spectral results showed no change of the SPR properties of these NPs after transfer to organic solvents. The TEM study also showed that the particle size and size distribution remain unchanged after transfer to organic solvent. The presence of an amino acid head group increases the thermal stability of the GNPs in either phase. This method can also be applied to the preparation of other MNPs by using a variety of amino acid derivatized fatty acid molecules. In brief, our method has several advantages over earlier reported methods, for example: 1) no external reducing agent is required; 2) 100% transfer occurs simply by changing the pH by using any protonated acid; 3) the nature and position of the SPR property of GNPs/SNPs remain unaltered during transfer; and 4) the method is very simple to use and requires only two steps.

## Experimental Section

**Materials:** Oleic acid, stearic acid, lauric acid, L-tryptophan (Trp), L-tyrosine (Tyr), dicyclohexylcarbodiimide (DCC), and 1-hydroxybenzotriazole (HOBt) were purchased from SRL India. Hydrogen tetrachloroaurate(III) trihydrate ( $\text{HAuCl}_4 \cdot 3\text{H}_2\text{O}$ ) and silver nitrate ( $\text{AgNO}_3$ ) were purchased from Sigma-Aldrich. All the aqueous solutions were made with triple-distilled water. HPLC-grade organic solvents were used for other purposes.

**Synthesis of redox-active amphiphiles:** Four new redox-active amphiphiles (conjugates of a fatty acid and an amino acid), oleic-Trp-COOH (Ole-Trp), stearic-Trp-COOH (Ste-Trp), lauric-Trp-COOH (Lau-Trp), and oleic-Tyr-COOH (Ole-Tyr), were synthesized by conventional solution-phase methods using a racemization-free fragmentation/condensation strategy.<sup>[59]</sup> Scheme 1 depicts the chemical structures of these tryptophan- and tyrosine-based redox-active amphiphiles. The C terminus of an amino acid was first protected by esterification with a methyl group, fol-

lowed by coupling with amphiphile by using DCC/HOBt. The details of the synthesis procedure and characterization of the products are provided in the Supporting Information. For CMC measurement, sodium salts of the corresponding amphiphiles were prepared by titration with sodium hydroxide in ethanol according to the literature report.<sup>[53]</sup>

**Preparation of amphiphile-capped gold nanoparticles (amphiphile-GNPs):** In a typical reaction, an amphiphile Ole-Trp/Ste-Trp/Lau-Trp/Ole-Tyr solution (1 mL, 40 mM in methanol) was diluted with triple-distilled water (8.5 mL). The pH of the medium was adjusted to alkaline by adding NaOH for complete solubilization of the amphiphile. An aqueous solution of  $\text{HAuCl}_4$  (0.5 mL, 10 mM) was then added dropwise to the above solution with constant magnetic stirring. The pH of the final reaction mixture was adjusted to  $\approx 11$  with standard NaOH solution, and

the mixture was stirred magnetically for 3 days at ambient temperature. We observed a color change from yellow to ruby red, indicating the formation of colloidal GNPs through oxidation of the tryptophan/tyrosine residue of the respective amphiphiles.

**Preparation of amphiphile-capped silver nanoparticles (amphiphile-SNPs):** In a typical reaction, an amphiphile Ole-Trp solution (1 mL, 40 mM in methanol) was dissolved in triple-distilled water (8.9 mL). The pH of the medium was adjusted to alkaline for complete solubilization of the amphiphile. An aqueous solution of  $\text{AgNO}_3$  (0.1 mL, 10 mM) was then added dropwise with constant magnetic stirring. The pH of the final reaction mixture was adjusted to  $\approx 11$  with standard NaOH solution, and the mixture was stirred for 3 days at room temperature. We observed a color change from colorless to yellow, indicating the formation of colloidal SNPs through oxidation of the tryptophan residue of the amphiphile.

**Preparation of oleic acid capped gold nanoparticles (oleic acid-GNPs):** In a typical reaction, oleic acid solution (1 mL, 40 mM in methanol) was dissolved in triple-distilled water (8 mL). The pH of the medium was adjusted to alkaline (pH 11) for complete solubility of oleic acid. An aqueous solution of  $\text{HAuCl}_4$  (0.5 mL, 10 mM) was added to the above solution with constant stirring. Finally,  $\text{NaBH}_4$  solution (0.5 mL, 10 mM) was added dropwise to the above mixture with constant magnetic stirring. A change of color from yellow to ruby red indicated the formation of oleate-stabilized GNPs and the solution was further stirred for 30 min.

**Phase transfer of amphiphile-GNPs and amphiphile-SNPs:** Typically, the as-prepared colloidal amphiphile-GNPs suspension (2 mL) was mixed with an equal volume of toluene to obtain two immiscible layers consisting of the transparent organic phase on the top and the colored hydrosol at the bottom. HCl (0.25 N) solution was added to this biphasic mixture under magnetic stirring to make the aqueous phase pH 2–3. The phase-transfer process was completed within a few minutes. The complete transfer of the GNPs from water to toluene can be visualized by the color change of the aqueous phase from ruby red to colorless, and at the same time the organic phase from colorless to ruby red. A similar procedure was also followed for the transfer of conjugates to other nonpolar organic solvents, such as benzene, xylene, cyclohexane, and hexane. The amphiphile-SNPs conjugates were also transferred to toluene by using the same procedures.

### Characterization

**NMR experiments:** All NMR studies of the redox-active amphiphiles in  $\text{CDCl}_3$  (1–10 mM) were carried out with Bruker DPX 300 MHz spectrometers. All NMR data are available in the Supporting Information.

**Determination of CMC of redox-active amphiphiles:** The CMC of the sodium salt of an amphiphile in water was determined by measuring the surface tension at 25°C by the ring method in a Krüss tensiometer. In a typical experiment, water (10 mL) was first placed in a glass container, which was equipped with a thermostatic water bath maintained at 25°C. The stock solution of a sodium salt of amphiphile (20 mM) was then added in small portions and the surface tension was recorded until a constant value was reached. Finally, surface tension was plotted against the amphiphile concentration. The CMC was then determined from the slope of the curve.

**UV/visible absorption spectroscopy:** UV/visible absorption spectra of the amphiphile-GNPs/SNPs suspension in both water and organic phase were recorded with a Hewlett Packard 8453 UV/visible spectrophotometer. For thermal stability studies of the colloidal amphiphile-GNPs/SNPs conjugates, the respective suspension was first placed in a 1 cm path-length quartz cuvette, which was then put in a cell holder equipped with a thermostatic water-circulation bath and the spectra were recorded at various temperatures. The upper temperature of the measurement was limited by the boiling point of the solvent or by the 80°C temperature limit of the bath.

**Transmission electron microscopy (TEM):** One drop of the as-prepared aqueous/toluene suspension of the amphiphile-GNPs/SNPs conjugates was placed on a carbon-coated copper grid and allowed to air dry. The grid was then observed under a JEOL JEM2010 high-resolution transmission electron microscope at an accelerating voltage of 200 kV.

**Fourier-transform IR (FTIR) spectroscopy:** FTIR spectra of neat Ole-Trp, neat sodium salt of Ole-Trp, and the centrifuged/washed/dried Ole-Trp-GNPs conjugates isolated from aqueous and toluene phases were recorded by a Shimadzu FTIR-8400S spectrometer. Pellets were prepared by mixing the corresponding dried sample with KBr in a 1:100 (wt/wt) ratio.

**Dynamic light scattering (DLS):** DLS data of the suspension of Ole-Trp-GNPs conjugates in water and in toluene were acquired with a Zetasizer Nano ZS apparatus (Malvern Instruments) containing a He-Ne laser operating at an incident wavelength of 652 nm.

**Thermogravimetric analysis (TGA):** The samples for TGA were isolated by ultracentrifugation of suspensions of the Ole-Trp-GNPs conjugates in water and in toluene. Thermograms of the dry powdered samples were recorded by using a TASDQ600 instrument at a heating rate of 20°C min<sup>-1</sup> under a N<sub>2</sub> atmosphere.

## Acknowledgements

S.S. thanks CSIR (India) for providing the fellowship. This research was supported by a grant (no. BT/PR3648/BRB/10/301/200) from DBT (India). Thanks are also due to the partial support from CSIR (grant no. 01(2105)/07/EMR-II) and the Nanoscience and Nanotechnology Initiatives, DST (India). We are also grateful to Prof. A. Dasgupta, University of Calcutta (India) for providing the DLS facility.

- [1] M.-C. Daniel, D. Astruc, *Chem. Rev.* **2004**, *104*, 293–346.
- [2] U. Kreibitz, M. Vollmer, *Optical Properties of Metal Clusters*, Springer, Berlin, **1995**.
- [3] C. J. Murphy, T. K. Sau, A. M. Gole, C. J. Orendorff, J. Gao, L. Gou, S. E. Hunyadi, T. Li, *J. Phys. Chem. B* **2005**, *109*, 13857–13870.
- [4] M. H. Rashid, R. R. Bhattacharjee, A. Kotal, T. K. Mandal, *Langmuir* **2006**, *22*, 7141–7143.
- [5] M. H. Rashid, R. R. Bhattacharjee, T. K. Mandal, *J. Phys. Chem. C* **2007**, *111*, 9684–9693.
- [6] M. Sastry, *Curr. Sci.* **2003**, *85*, 1735–1745 and references therein.
- [7] M. P. Andrews, G. A. Ozin, *J. Phys. Chem.* **1986**, *90*, 2929–2938.
- [8] Y. Nakao, K. Kaeriyama, *J. Colloid Interface Sci.* **1989**, *131*, 186–191.
- [9] P. Mulvaney, *Langmuir* **1996**, *12*, 788–800.
- [10] S. Efrima, *Heterog. Chem. Rev.* **1994**, *1*, 339–353.

- [11] W. Wang, X. Chen, S. Efrima, *J. Phys. Chem. B* **1999**, *103*, 7238–7246.
- [12] W. Wang, S. Efrima, O. Regev, *Langmuir* **1998**, *14*, 602–610.
- [13] W. Wang, S. Efrima, O. Regev, *J. Phys. Chem. B* **1999**, *103*, 5613–5621.
- [14] M. Brust, M. Walker, D. Bethell, D. J. Schiffrin, R. Whyman, *J. Chem. Soc. Chem. Commun.* **1994**, 801–802.
- [15] L. O. Brown, J. E. Hutchinson, *J. Phys. Chem. B* **2001**, *105*, 8911–8916.
- [16] M. Green, *Chem. Commun.* **2005**, 3002–3011 and references therein.
- [17] X. Z. Lin, X. Teng, H. Yang, *Langmuir* **2003**, *19*, 10081–10085.
- [18] K. Esumi, T. Tano, K. Meguro, *Langmuir* **1989**, *5*, 268–270.
- [19] K. Esumi, T. Tano, K. Torigoe, K. Meguro, *Chem. Mater.* **1990**, *2*, 564–567.
- [20] F. Wen, N. Waldöfner, W. Schmidt, K. Angermund, H. Bönemann, S. Modrow, S. Zinoveva, H. Modrow, J. Hormes, L. Beuermann, S. Rudenkiy, W. Maus-Friedrichs, V. Kempter, T. Vad, H.-G. Haubold, *Eur. J. Inorg. Chem.* **2005**, 3625–3640.
- [21] D. V. Leff, P. C. Ohara, J. R. Heath, W. M. Gelbart, *J. Phys. Chem.* **1995**, *99*, 7036–7041.
- [22] R. L. Whetten, J. T. Khoury, M. M. Alvarez, S. Murthy, I. Vezmar, Z. L. Wang, P. W. Stephens, C. L. Cleveland, W. D. Luedtke, U. Landman, *Adv. Mater.* **1996**, *8*, 428–433.
- [23] S. R. Johnson, S. D. Evans, S. W. Mahon, A. Ulman, *Langmuir* **1997**, *13*, 51–57.
- [24] K. S. Mayya, V. Patil, M. Sastry, *Langmuir* **1997**, *13*, 3944–3947.
- [25] D. V. Leff, L. Brandt, J. R. Heath, *Langmuir* **1996**, *12*, 4723–4730.
- [26] K. S. Mayya, F. Caruso, *Langmuir* **2003**, *19*, 6987–6993.
- [27] L. A. Porter, D. Ji, S. L. Westcott, M. Graupe, R. S. Czernuszewicz, N. J. Halas, T. R. Lee, *Langmuir* **1998**, *14*, 7378–7386.
- [28] J. Liu, R. Xu, A. E. Kaifer, *Langmuir* **1998**, *14*, 7337–7339.
- [29] J. Liu, S. Mendoza, E. Roman, M. J. Lynn, R. Xu, A. E. Kaifer, *J. Am. Chem. Soc.* **1999**, *121*, 4304–4305.
- [30] K. V. Sarathy, G. U. Kulkarni, C. N. R. Rao, *Chem. Commun.* **1997**, 537–538.
- [31] P. R. Selvakannan, S. Mandal, R. Pasricha, S. D. Adyanthaya, M. Sastry, *Chem. Commun.* **2002**, 1334–1335.
- [32] J. Yang, J. Y. Lee, T. C. Deivaraj, H.-P. Too, *J. Colloid Interface Sci.* **2004**, *277*, 95–99.
- [33] J. M. McMahon, S. R. Emory, *Langmuir* **2007**, *23*, 1414–1418.
- [34] E. R. Zubarev, J. Xu, A. Sayyad, J. D. Gibson, *J. Am. Chem. Soc.* **2006**, *128*, 15098–15099.
- [35] M. Aslam, I. S. Mulla, K. Vijayamohan, *Langmuir* **2001**, *17*, 7487–7493.
- [36] C. N. R. Rao, G. U. Kulkarni, P. J. Thomas, V. V. Agrawal, P. Saravanan, *J. Phys. Chem. B* **2003**, *107*, 7391–7395.
- [37] S. Underwood, P. Mulvaney, *Langmuir* **1994**, *10*, 3427–3430.
- [38] M. J. Hostetler, S. J. Green, J. J. Stokes, R. W. Murray, *J. Am. Chem. Soc.* **1996**, *118*, 4212–4213.
- [39] R. S. Ingram, M. J. Hostetler, R. W. Murray, *J. Am. Chem. Soc.* **1997**, *119*, 9175–9178.
- [40] S. Rucareanu, V. J. Gandubert, R. B. Lennox, *Chem. Mater.* **2006**, *18*, 4674–4680.
- [41] M. Sastry, A. Kumar, P. Mukherjee, *Colloids Surf. A: Physicochem. Eng. Aspects* **2001**, *181*, 255–259.
- [42] A. Kumar, P. Mukherjee, A. Guha, S. D. Adyanthaya, A. B. Mandale, R. Kumar, M. Sastry, *Langmuir* **2000**, *16*, 9775–9783.
- [43] K. V. Sarathy, G. Raina, R. T. Yadav, G. U. Kulkarni, C. N. R. Rao, *J. Phys. Chem. B* **1997**, *101*, 9876–9880.
- [44] T. Bala, A. Swami, B. L. V. Prasad, M. Sastry, *J. Colloid Interface Sci.* **2005**, *283*, 422–431.
- [45] Y. Zhou, W. Chen, H. Itoh, K. Naka, Q. Ni, H. Yamane, Y. Chujo, *Chem. Commun.* **2001**, 2518–2519.
- [46] J. M. Slocik, R. R. Naik, M. O. Stone, D. W. Wright, *J. Mater. Chem.* **2005**, *15*, 749–753.
- [47] J. M. Slocik, M. O. Stone, R. R. Naik, *Small* **2005**, *1*, 1048–1052.



- [48] P. R. Selvakannan, S. Mandal, S. Phadtare, A. Gole, R. Pasricha, S. D. Adyanthaya, M. Sastry, *J. Colloid Interface Sci.* **2004**, 269, 97–102.
- [49] S. Si, T. K. Mandal, *Chem. Eur. J.* **2007**, 13, 3160–3168.
- [50] S. Si, R. R. Bhattacharjee, A. Banerjee, T. K. Mandal, *Chem. Eur. J.* **2006**, 12, 1256–1265.
- [51] R. R. Bhattacharjee, A. K. Das, D. Haldar, S. Si, A. Banerjee, T. K. Mandal, *J. Nanosci. Nanotechnol.* **2005**, 5, 1141–1147.
- [52] A. Swami, A. Kumar, M. D'Costa, R. Pasricha, M. Sastry, *J. Mater. Chem.* **2004**, 14, 2696–2702.
- [53] B. D. Flockhart, H. Graham, *J. Colloid Sci.* **1953**, 8, 105–115.
- [54] J. A. Creighton, D. G. Eadon, *J. Chem. Soc. Faraday Trans.* **1991**, 87, 3881–3891.
- [55] A. Okugaichi, K. Torigoe, T. Yoshimura, K. Esumi, *Colloids Surf. A: Physicochem. Eng. Aspects* **2006**, 273, 154–160.
- [56] S. Si, T. K. Mandal, *Langmuir* **2007**, 23, 190–195.
- [57] X. Yang, S. S. Perry, *Langmuir* **2003**, 19, 6135–6139.
- [58] C. D. Bain, E. B. Troughton, Y.-T. Tao, J. Evall, G. M. Whitesides, R. G. Nuzzo, *J. Am. Chem. Soc.* **1989**, 111, 321–335.
- [59] M. Bodanszky, A. Bodanszky, *The Practice of Peptide Synthesis*, 2nd revised ed., Springer, Berlin, **1994**.

Received: July 3, 2007

Published online: October 24, 2007